Characterization of InP:Fe Charged Particle Tracking Detectors

Earl Russell Tang Almazan*
Jason Nielsen* and Michael Hance*
*Santa Cruz Institute for Particle Physics, University of California at Santa Cruz

I. Introduction

Silicon trackers are commonly used in HEP experiments. However, modern silicon detector manufacturing results in logistical bottlenecks and high costs. Thin film techniques offer potential improvements on existing detector fabrication methods with scalable production. Thin film technologies are used to produce a variety of products, from solar panels to PCBs to LCD screens. Existing commercial equipment could then be used to produce bulk monolithic detectors on flexible substrates. The Thin Films collaboration between UC Santa Cruz and Argonne aims to develop charged particle tracking detectors with promising materials.

HEP applications for thin films are currently in their infancy. Demonstrating this technology requires fabricating prototype detectors from materials amenable to thin-film fabrication with favorable properties for charged particle detection. Indium phosphide doped with iron (InP:Fe) was chosen for its high electron mobility and high resistivity compared to silicon. Iron doping reduces the number of mobile charge carriers, thereby increasing the bulk resistivity of the material from an n-type semiconductor to a semi-insulator. Basic devices were fabricated at Argonne National Lab (ANL) with a uniform thick layer of InP:Fe between two conducting plates (Figure 1a). Monocrystalline wafers were used to fabricate devices for InP:Fe characterization. Using the first prototype set of devices, colleagues in ANL were able to determine leakage current and charged particle response at differing temperatures from InP:Fe. Further material properties were determined from a second generation of devices, manufactured at ANL and delivered to the Santa Cruz Institute for Particle Physics (SCIPP), located in University of California Santa Cruz (UCSC).

With the aid of HEPCAT funding my full-time employment in the Thin Films collaboration, my main focus has been characterizing InP:Fe. Basic electrical tests (I-V and C-V) were used to determine leakage current, sensor material composition, breakdown voltage, and inter-device uniformity. Studying the transient response of InP:Fe to charged particles (Sr-90), infrared light, and red laser light helps differentiate charge carrier responses and identify transient waveform properties. X-ray test beams at CLS and DLS enabled measuring both active area uniformity and unexpected photo-induced behavior.

II. Electrical Tests

Leakage current properties and breakdown voltage were determined through I-V tests. A boundary between ohmic and non-ohmic leakage current behavior was found at approximately 350 V (Figure 2a). Leakage current uniformity across devices can be summarized by a roughly constant 0.1 Relative Standard Deviation (RSD) from -600 to 600 V applied voltage, suggesting inter-device leakage current variance is proportional to the leakage current magnitude (Figure 2b). Since the InP:Fe layer is uniformly doped, the magnitude of leakage current is expected to be independent of the polarity of applied voltage. Figure 2a agrees with this hypothesis. Using one device as a test, 1 kV was determined as a reasonable estimate of the breakdown voltage.

Voltage-dependent capacitance behavior can be derived from C-V tests with AC power supply frequencies ranging from 1 MHz to 1kHz. At 1 MHz, the floating-guard-ring capacitance remained constant at 2.1 pF from -20 to 20 applied voltage. Lowering the frequency to 1kHz results in higher overall capacitance and observed voltage dependence (Figure 2d). Grounding device guard rings during C-V measurements lowers both the overall capacitance and the dependence of capacitance on applied voltage.

Devices were identified with higher than expected leakage current at low positive applied voltage, hereafter coined as the high-current devices. The high-current devices also exhibited high capacitance at high positive applied voltage, mimicking C-V behavior seen in MOS capacitor devices. Testing whether the same phenomena in MOS capacitors is the same that is affecting InP devices is ongoing. The variant I-V behavior shown in high-current devices is less relevant at higher applied voltages, where the variance of leakage current values from RSD_{leak} dominates. These devices were spatially close to one another before being diced and separated from the initial wafer, suggesting the cause of high leakage current is from a physical defect in the original wafer before being broken apart (Figure 2c).

III. Sr-90, Infrared Laser, and Red Laser Transient Response

Device behavior from low-energy sources was investigated using a device exhibiting I-V and C-V that was standard compared to the full InP:Fe set. This device was mounted on a standard 1-ch UCSC board without optimizing for better SNR or pulse shaping.

The charged-MIP response of InP:Fe was observed using a collimated beam of 0.546 MeV electrons, emitted by Sr-90, to induce transient signals at a range of applied voltages. The

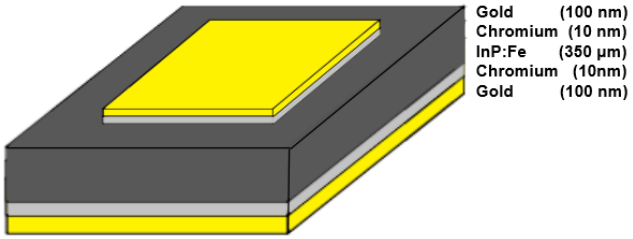

(a) Device Cross-Section Diagram

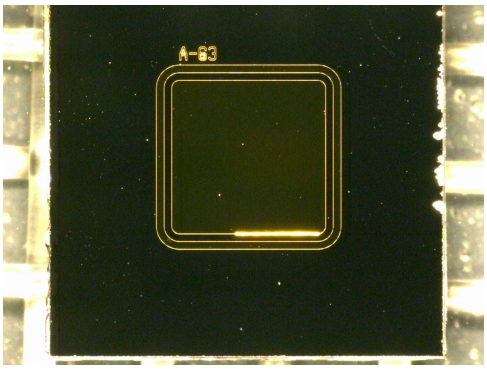

(b) Device A63_NH

Fig. 1: 48 devices were diced from an initial 2 inch radius commercial InP:Fe wafer in 5 mm by 5 mm squares. Backside metallization was deposited uniformly, while topside metallization was patterned in the shape displayed in Figure 1b, consisting of a 2 by 2 mm^2 central pad with rounded corners and a 100 μm thick guard ring, spaced from the central pad by a 100 μm gap.

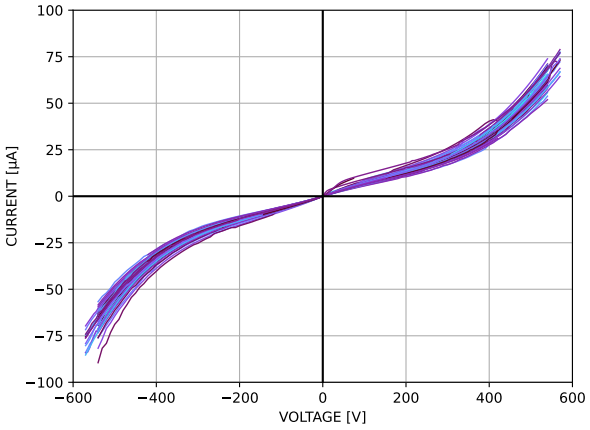

(a) I-V measurements were taken for all 48 devices, with all I-V curves superimposed on one another in this plot.

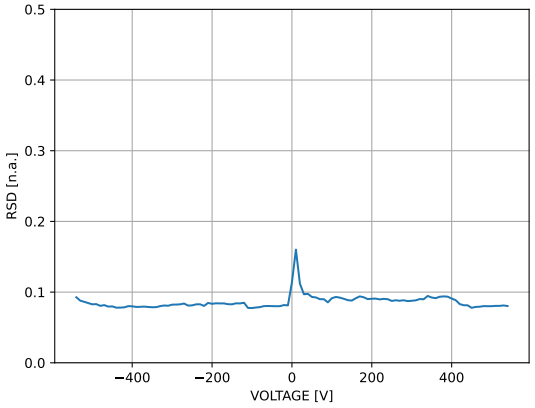

(b) Leakage Current Relative Standard Deviation (RSD$_{leak}$) is defined as leakage current standard deviation divided by the average leakage current magnitude. This value is calculated at each applied voltage.

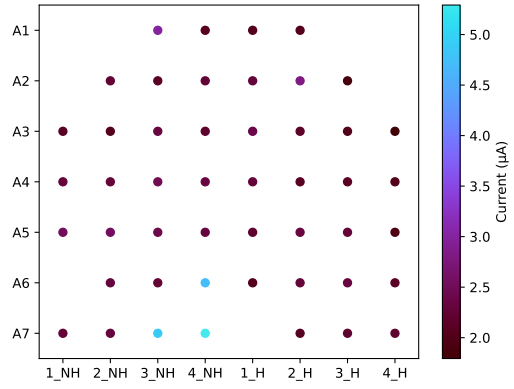

(c) All 48 devices are arranged by their past positions in the original wafer, before dicing, color coded by their leakage current at +30 V. High current devices visible in lower middle of the plot.

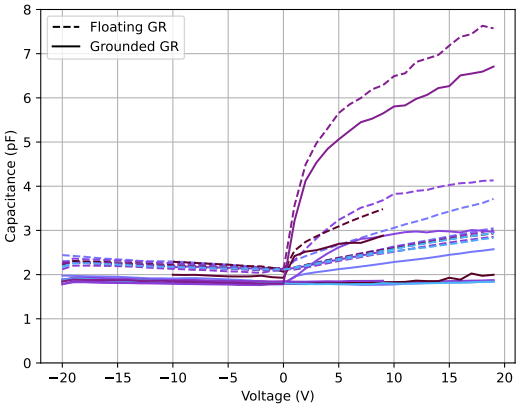

(d) C-V measurements of 30 devices at 1 kHz. Each line represents a distinct device's C-V measurement. Dashed lines are C-V measurements taken with a floating guard ring, while solid lines are those taken with a grounded guard ring.

Fig. 2: Plots for Electrical Tests

averaged waveforms per voltage were taken, not the raw waveforms (Figure 3b). This data set was used to evaluate trends in charged-MIP transient response behavior as a function of applied voltage.

Uncharged MIP response and position reconstruction studies were attempted with an infrared beam, attenuated to allow single photons for transient response measurements. However, since InP:Fe was found to be transparent to infrared light, a 632 nm red laser is used instead. In addition, the non-uniform deposition of energy from red laser photons results in the majority of primary charge carriers originating from near the topside layer. The main charge carrier flowing through the device and producing the transient signal is determined by the polarity of applied voltage. When the voltage applied to the backside is positive, electrons move from the topside layer to the backside.

The higher response from positive applied voltages agrees with the higher electron carrier mobility, compared to the hole carrier mobility, in InP:Fe (Figure 3a). Positive applied voltage waveforms also appear to have a secondary tail after the initial peak, identified from 15 to 70 ns. Primary holes could not be responsible for the tail, as the negative polarity waveform does not match the shape nor duration of the positive polarity tail. Identifying why the positive polarity tail exists is under ongoing investigation.

Despite the absence of any dedicated architecture or equipment made for reducing noise or improving the signal, both the transient electron and red laser responses showed fast, clear pulses on the order of nanoseconds.

IV. Probing Active Area Properties Using Focused X-Rays

The Thin Films group collaborated with TRIUMF used photocurrent variance from focused x-ray scans to measure material variance in monocrystalline wafers. This measurment serves as a baseline for determining the uniformity of InP:Fe as a material before considering the impact of thin-film production methods. At both Diamond Light Source (DLS) and Canadian Light Source (CLS), two devices were characterized. Due to both tests were performed at 15 keV beam energy, similar to the red laser tests, the majority of the beam energy is deposited in the initial 15% depth into the material. Conclusions reached from both test beams then should be interpreted as a shallow depth probe of intra-device uniformity. The main difference between tests at both facilities is the beam width: the 2 μm DLS beam width is narrower than the 20 μm CLS beam width.

X-ray scans were separated into two spatial region types: those without photocurrent across scans (background regions) and those that have photocurrent in at least one scan (active regions). Non-photocurrent background-region currents were modelled as linear fits to background-region data. Non-photocurrent active-region currents were modelled as a linear continuation between the backround-regions surrounding the active region (Figure 4a). The photocurrent is interpreted as the raw data minus these linear non-photocurrent fits. From here, the photocurent is evaluated for magnitude, width, and under-central-pad uniformity as a function of applied voltage.

At CLS, the initial probe into intra-device uniformity was hampered by an unreliable thermocouple during testing, leaving results difficult to interpret as either phenomena worth reviewing or the result of temperature fluctuations. In addition, measured currents fluctuated wildly at applied voltages higher than +50 V. This informed improvements to the experiment at DLS: a working thermocouple and passive heat dissipation were implemented on the DLS board to eliminate errors from temperature fluctuations.

At DLS, photocurrents measured were stable enough to record photocurrent properties across a wide applied voltage range for Device 2 (Figure 4b). Temperature fluctuations on the order of 0.5 C measured at DLS disqualifies temperature changes as being responsible for phenomena beyond noise. Because of this, unforseen behaviors seen in both CLS and DLS cannot be due to temperature fluctuations: the 'dip', 'sideband decay', and 'flare-up' phenomena.

'Flare-up' refers to the high-currents identified outside of the central pad region of, but still on, Device 2 at CLS (Figure 5a). This phenomenon initiated questions on whether leakage current thermal runaway is responsible, as the 'flare-up' occurred chronologically after the scan passed over the central pad region. Poor temperature measurements meant verifying or disproving this hypothesis is not possible.

The 'dip' is a physical region in Device 1 in DLS that, when hit with the DLS test beam, showed a photocurrent with constant polarity independent of applied voltage polarity (Figure 5b). This behavior was not observed in other devices at DLS and CLS, so regions scanning over the dip were not included in assessing device uniformity. Given the dip was located in the central pad region, with a large width near equal to the central pad width, Device 1 suffers from low statistics.

'Sideband decay' is the observed phenomena of photocurrents persisting for several seconds after xray stimulation at DLS (Figure 5c). From +400 V x-ray scans of DLS Device 2, sideband decay closely follows an exponentially decreasing photocurrent after the beam is taken off of the active area. This behavior also appears to persist between 400 V scans, suggesting this phenomena persists for several minutes after an initial photoresponse.

V. Near-Future Plans

The Thin Films collaboration is in the process of drafting papers, aiming to publish within this year. Further characterization of InP:Fe is currently underway. The two main areas of study being pursued are studies of irradiated samples and anomalous x-ray response characterization.

The arrival of neutron-irradiated InP:Fe samples has enabled work on the effect of radiation on InP:Fe I-V, C-V, Sr-90 MIP response, uniformity, and charge collection efficiency (CCE). Twelve devices had been sent to Ljubljana for neutron irradiation at fluences ranging from 10^{13} to 10^{16} n_{eq}/cm^2 in logarithmic steps. Only devices which have experienced 10^{13} and 10^{14} n_{eq}/cm^2 fluences have returned, with devices under higher fluences still at Ljubljana. I-V and C-V have already been measured for irradiated devices, with annealing tests and CCE measurements anticipated for the near future. Temperature dependent I-V, C-V, and MIP response measurements

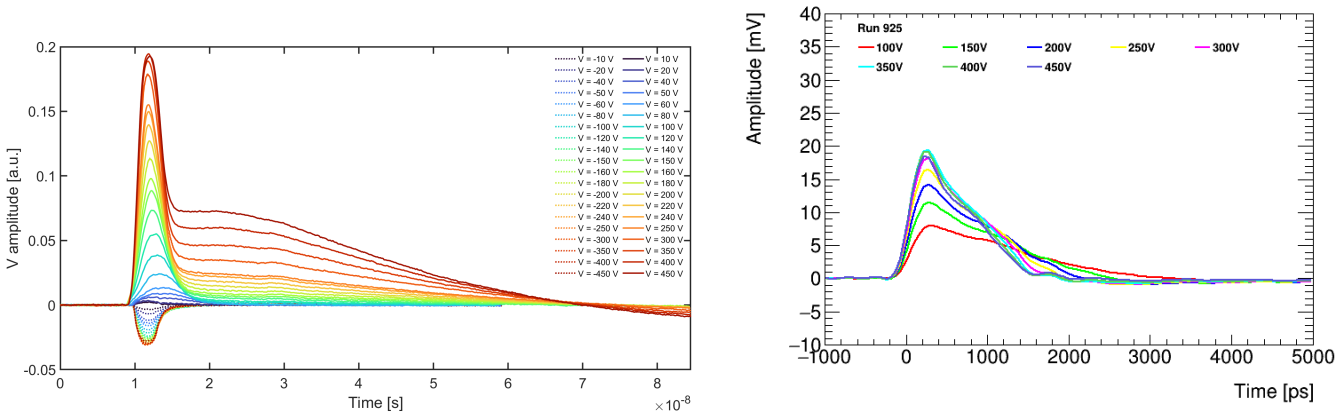

(a) Red Laser

(b) Sr-90 Electrons

Fig. 3: Transient Waveforms

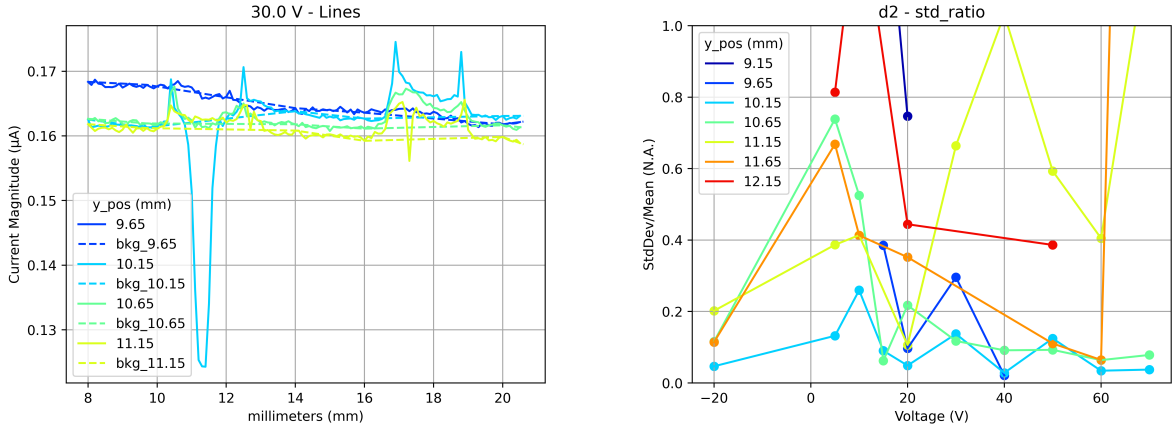

(a) DLS Raw Currents
+30 V

(b) DLS Device 2
Central Pad RSD vs Voltage

Fig. 4: Photocurrent uniformity as a function of x-ray beam position was measured as a proxy for intra-device uniformity. The central pad in line scans span from 10 to 12 mm in the y-axis. For this reason, lines in Figure 4b beyond this range should not be interpreted as indicative of intra-device active area uniformity. Measurements from 0 to 20 V may be unreliable due to low S/N.

are currently in progress for irradiated devices as well. For CCE measurements, an Alibava DAQ system is currently being refurbished in-house with expected measurements by the end of Spring. A thermography station is also under construction, utilizing a Thorlabs thermal camera to assess device uniformity while devices are powered.

A DLS x-ray test beam is currently being planned for Winter of this year to characterize the sideband decay and dip phenomena detailed in Section IV. The test beam energy will also be increased to address the low penetration depth of the 15 keV energy set in both previous test beams.

VI. Long Term Plans

While the existing batch of crystalline InP:Fe devices serve as a baseline for the characterizing InP:Fe, the next step is to fabricate devices using chemical vapor deposition and characterize the change in performance as a result of the new manufacturing method. Once this is complete, the viability of InP:Fe can be fully evaluated as a candidate material in thin-film charged particle tracking detectors. The information gained from characterization, both completed and near-future, will be used to inform the architecture of the next generation of devices.

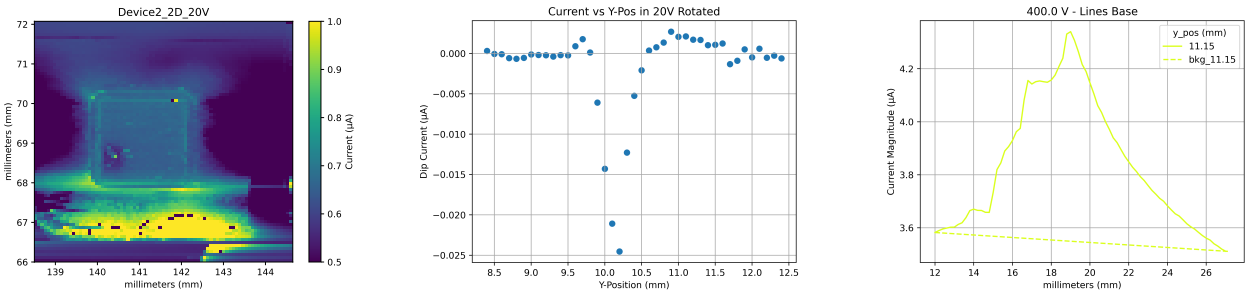

(a) Flare-Up (b) Dip Current (c) Sideband Decay

Fig. 5: Unexpected phenomena identified at CLS and DLS